Inclusive and exclusive quasielastic $\vec{p}+{}^2\mathrm{H}$ spin observables at 647 and 800 MeV

M. L. Barlett, G. W. Hoffmann, L. Ray, G. Pauletta,* and K. H. McNaughton
Department of Physics, The University of Texas at Austin, Austin, Texas 78712

J. F. Amann, K. W. Jones, J. B. McClelland, and M. W. McNaughton
Los Alamos National Laboratory, Los Alamos, New Mexico 87545

R. Fergerson†
Department of Physics, Rutgers University, Piscataway, New Jersey 08855

D. Lopiano‡
Department of Physics, University of California at Los Angeles, Los Angeles, California 90024
(Received 14 August 1989)

Inclusive quasielastic $\vec{p}+{}^2\mathrm{H}$ analyzing-power and spin-rotation depolarization (D_{ij}) data are reported for the nucleon-nucleon center-of-momentum angular ranges 46.9°–118.0° and 58.3°–110.0° at 647 and 800 MeV, respectively. Exclusive quasielastic $\vec{p}\vec{p}$ and $\vec{p}n$ analyzing-power data and exclusive $\vec{p}\vec{p}$ D_{ij} data are also presented. A simple isospin weighting model successfully describes the inclusive data and is used to estimate the free $\vec{p}n$ D_{ij} values. The new data are compared with those of previous experiments and with predictions of phase-shift analyses. The deduced $\vec{p}n$ D_{ij} values extend the angular range of previous 800 MeV data and provide entirely new information at 647 MeV.

I. INTRODUCTION

A variety of intermediate-energy proton-proton (pp) and proton-neutron (pn and np) experiments have been performed in recent years. The amount of data now available for characterizing the $I=1$ part of the nucleon-nucleon (NN) elastic scattering amplitude is impressive; recent phase-shift analyses[1] lead to the conclusion that the pp scattering amplitudes are well determined at energies below 1 GeV.

The pn and np data sets available for investigations of the $I=0$ part of the NN interaction are more sparse[1] and of poorer quality than the comparable pp data. A significant fraction of this data base is for pn quasielastic

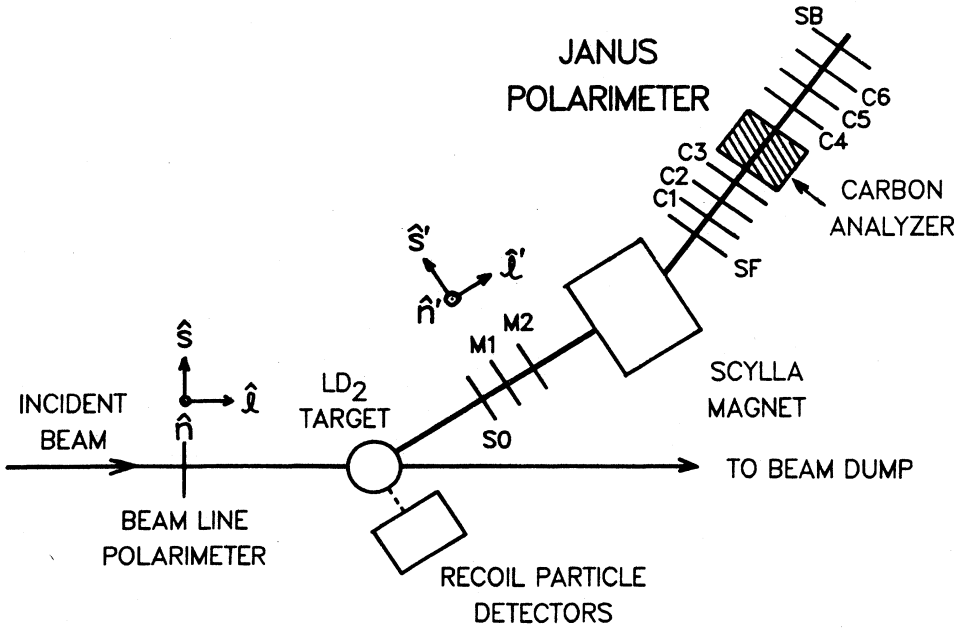

FIG. 1. A schematic drawing of the experimental setup showing the major components. Scintillators *SO*, *SF*, and *SB* form the event trigger. $M1$ and $M2$ are multiwire proportional chambers while $C1$–$C6$ are multiwire drift chambers. The coordinate systems shown for the incident- and scattered-particle frames are consistent with the equations in the text.

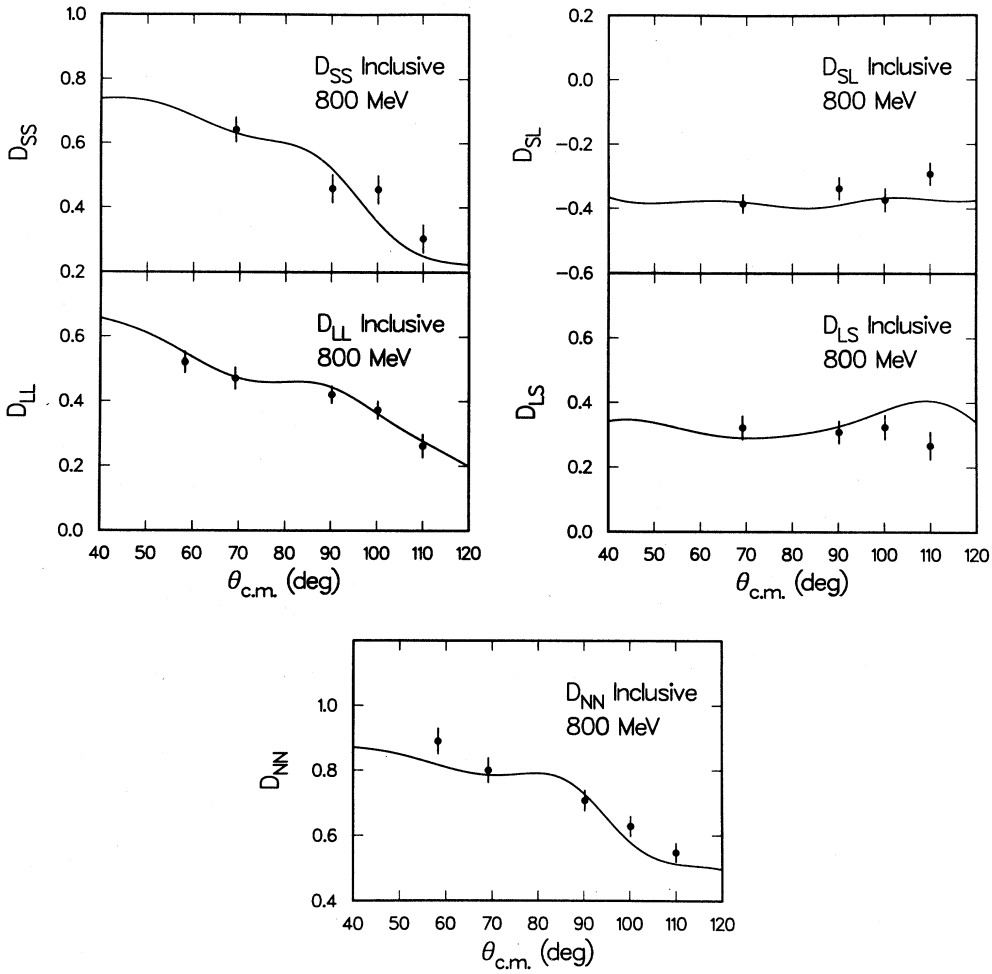

FIG. 2. The spin-rotation depolarization parameters, D_{ij}, for inclusive quasielastic $\vec{p}+{}^2\mathrm{H}$ scattering at 800 MeV. The solid curves indicate predictions of the isospin weighting model. The c.m. angles refer to *NN* kinematics as discussed in the text.

scattering from deuterium. In fact, if these quasielastic measurements are excluded, only cross section, analyzing power/polarization, and a few spin-correlation data sets remain for center-of-mass (c.m.) angles *smaller* than 90° and energies above 500 MeV.[1–3] Yet the forward angular range is precisely the region where well determined *pn* scattering amplitudes are required as first-order input for proton-nucleus scattering models[4–7] (both relativistic and nonrelativistic). Quasielastic *pn* data are, for the time being, an indispensable part of the *pn* data base and it is therefore important to continue carrying out such measurements. At the same time it is well advised to check the reliability of the quasielastic data by comparing them where possible with free *NN* elastic data.

Here we present results of 800 MeV $\vec{p}+{}^2\mathrm{H}$ inclusive quasielastic analyzing-power and spin-rotation depolarization (D_{ij}) measurements, exclusive quasielastic $\vec{p}p$ analyzing-power and D_{ij} measurements, and exclusive quasielastic $\vec{p}n$ analyzing-power measurements for the center-of-momentum angular range $58.3° \leq \theta_{\mathrm{c.m.}} \leq 110.0°$. Similar data at 647 MeV for the angular range $46.9° \leq \theta_{\mathrm{c.m.}} \leq 118.0°$ are also reported. We compare free *pp* elastic and exclusive *pp* quasielastic spin observable data at 800 MeV at larger angles than was done in Ref. 8; a similar comparison is given at 647 MeV. We also investigate the extent to which reasonable estimates of the free *pn* spin observables can be obtained from inclusive quasielastic $\vec{p}+{}^2\mathrm{H}$ scattering data, given accurate values for the free *pp* spin observables, using a simple isospin weighting model. Measurements were made at 647 MeV in order to provide data at an intervening energy between 500 and 800 MeV. At 500 MeV quasielastic *pn* analyzing-power (A_y) and D_{ij} data were found to be in good agreement with predictions of phase-shift analyses[9] whereas this was not the case at 800 MeV.[8]

Details of the experiment are briefly discussed in the next section. The off-line data analysis is explained and the results presented in Sec. III. Experimental errors are explained in Sec. IV, while the summary and conclusions are given in Sec. V.

II. EXPERIMENTAL

The experiment was done at the external proton beam (EPB) experimental area of the Los Alamos Clinton P. Anderson Meson Physics Facility (LAMPF). Beams of 647 and 800 MeV polarized protons ($\hat{n}$, $\hat{s}$, and $\hat{l}$; see Fig. 1 for coordinate system definitions) were incident on a 7.6 cm diam liquid deuterium target. The magnitude and direction of the incident-beam polarization were monitored using a beam line polarimeter located upstream of the target and a set of quench monitors.[10] Beam polarization was typically 70–80% during the course of the experiment. For each type of beam, normal (+) and reverse (−) directions [$\hat{n}$: up (+), down (−); $\hat{s}$: left (+), right (−); $\hat{l}$: parallel (+), antiparallel (−) to incident momentum] were changed at the ion source every minute. Logic levels from the source were read by the on-line data acquisition system and used to tag each event according to beam spin orientation.

Scattered protons were detected and momentum analyzed using the arrangement shown in Fig. 1. A threefold coincidence among scintillators *SO*, *SF*, and *SB* (see Fig. 1) defined the event trigger. Particle identification was accomplished via *SO* pulse height and time-of-flight between *SO* and *SF*. Trajectories after scattering were determined using sets of multiwire proportional chambers (MWPC's) $M1$ and $M2$. The SCYLLA magnet (see Fig. 1) served as both low-resolution spectrometer ($\Delta p/p \simeq 1-3\%$) and spin precessor. Upon exiting the magnet, the particles were analyzed using the JANUS polarimeter (see Fig. 1).

JANUS consists of six sets of multiwire drift chambers (MWDC's), an adjustable thickness carbon analyzer, and trigger scintillators *SF* and *SB*. Initial particle trajectories were determined using MWDC's $C1-C3$. The carbon analyzer rescattered the protons and final trajectories were determined using MWDC's $C4-C6$. For each event trigger, a microprogrammable branch driver (MBD), which interfaced the CAMAC system to a VAX 11/750 computer, performed fast tests on the MWDC data to determine a crude polar scattering angle. Events which corresponded to scattering at small angles in the carbon analyzer ($\theta_C \leq 3°$) were cleared from the data stream; events passing the MBD test were taped and a

TABLE I. Inclusive quasielastic $\vec{p}+{}^2$H spin-rotation and -depolarization parameters at 800 MeV.

θ_{lab} (deg)	$\theta_{c.m.}$ (deg)	D_{NN}	ΔD_{NN}
25.0	58.3	0.890	±0.041
30.0	69.2	0.800	0.039
40.0	90.2	0.707	0.033
45.0	100.2	0.628[a]	0.032[a]
50.0	110.0	0.547	0.030

θ_{lab} (deg)	$\theta_{c.m.}$ (deg)	D_{SS}	ΔD_{SS}
30.0	69.2	0.643	±0.040
40.0	90.2	0.459	0.045
45.0	100.2	0.456	0.046
50.0	110.0	0.304	0.045

θ_{lab} (deg)	$\theta_{c.m.}$ (deg)	D_{SL}	ΔD_{SL}
30.0	69.2	−0.386	±0.030
40.0	90.2	−0.339	0.036
45.0	100.2	−0.374	0.037
50.0	110.0	−0.293	0.036

θ_{lab} (deg)	$\theta_{c.m.}$ (deg)	D_{LL}	ΔD_{LL}
25.0	58.3	0.521	±0.034
30.0	69.2	0.471	0.035
40.0	90.2	0.421	0.028
45.0	100.2	0.373	0.029
50.0	110.0	0.262	0.037

θ_{lab} (deg)	$\theta_{c.m.}$ (deg)	D_{LS}	ΔD_{LS}
30.0	69.2	0.322	±0.038
40.0	90.2	0.309	0.036
45.0	100.2	0.324	0.039
50.0	110.0	0.267	0.044

[a]Calculated using $A_y = -0.240 \pm 0.010$ from SP87 phase shifts and isospin weighting model.

TABLE II. Inclusive quasielastic $\vec{p}+{}^2$H spin-rotation and -depolarization parameters at 647 MeV.

θ_{lab} (deg)	$\theta_{c.m.}$ (deg)	D_{NN}	ΔD_{NN}
20.5	46.9	0.899	±0.043
25.0	56.9	0.778	0.045
30.0	67.7	0.769	0.043
35.0	78.3	0.825	0.072
40.0	88.6	0.706	0.046
45.0	98.6	0.604	0.043
50.0	108.4	0.564	0.043
55.0	118.0	0.451	0.054

θ_{lab} (deg)	$\theta_{c.m.}$ (deg)	D_{SS}	ΔD_{SS}
20.5	46.9	0.687	±0.055
35.0	78.3	0.532	0.044
40.0	88.6	0.478	0.040
50.0	108.4	0.285	0.037

θ_{lab} (deg)	$\theta_{c.m.}$ (deg)	D_{SL}	ΔD_{SL}
20.5	46.9	−0.513	±0.040
35.0	78.3	−0.465	0.039
40.0	88.6	−0.395	0.032
50.0	108.4	−0.202	0.028

θ_{lab} (deg)	$\theta_{c.m.}$ (deg)	D_{LL}	ΔD_{LL}
20.5	46.9	0.543	±0.040
35.0	78.3	0.482	0.037
40.0	88.6	0.412	0.035
50.0	108.4	0.209	0.036

θ_{lab} (deg)	$\theta_{c.m.}$ (deg)	D_{LS}	ΔD_{LS}
20.5	46.9	0.517	±0.047
35.0	78.3	0.473	0.042
40.0	88.6	0.337	0.037
50.0	108.4	0.087	0.063

sample was analyzed on line by the VAX as time permitted. Asymmetries and particle polarizations were computed utilizing the inclusive 500 MeV $\vec{p}+{}^{12}C$ analyzing power, the polar distribution,[11] and the azimuthal distributions determined from particle trajectories.[12,13] Analyzer thickness was chosen as a function of incident-particle energy in order to minimize multiple Coulomb scattering while maintaining a reasonable figure of merit (σA_y^2). Details of JANUS design and operation are given in Refs. 12 and 14.

A recoil particle detector system allowed exclusive measurements to be made. The recoil system consisted of a 2×2 array of scintillators (7.5 cm ×7.5 cm ×15 cm) and two thin (19 cm ×9 cm ×0.6 cm) scintillators (used to tag charged recoils) positioned between the array and the target. Pulse-height information from the photomultipliers coupled to these detectors was recorded using analog-to-digital converters (ADC's). Fast timing signals from the detector anodes provided stop times for time-to-digital converters (TDC's). The start time was taken from the event trigger signal (SO·SF·SB). The relative time between the trigger and recoil events was recorded and used to separate the time correlated events from the random coincidence background. For each scattering angle the recoil system was positioned at the appropriate conjugate angle for free *NN* scattering.

Monitor events (typically 1 in every 20) were written to tape regardless of the outcome of the MBD test; these data provided an unbiased sample of events for monitoring and efficiency determinations. The monitor events were also used to obtain the inclusive $\vec{p}+{}^2H$ analyzing powers and the 647 MeV quasielastic $\vec{p}p$ and $\vec{p}n$ analyzing powers.

Finally, since the magnetic field of SCYLLA is vertical, spin precession mixes the components of polarization which lie in the bend plane ($\hat{s}$ and $\hat{l}$). To decouple these components and determine the D_{ij}'s requires measurement of the outgoing horizontal polarization component for two different precession angles. The precession of the bend-plane polarization components is proportional to the bend angle; thus for the $\hat{s}$- and $\hat{l}$-type beam runs data were taken using SCYLLA with fields corresponding to outgoing horizontal precessions of approximately 90° and 30°.

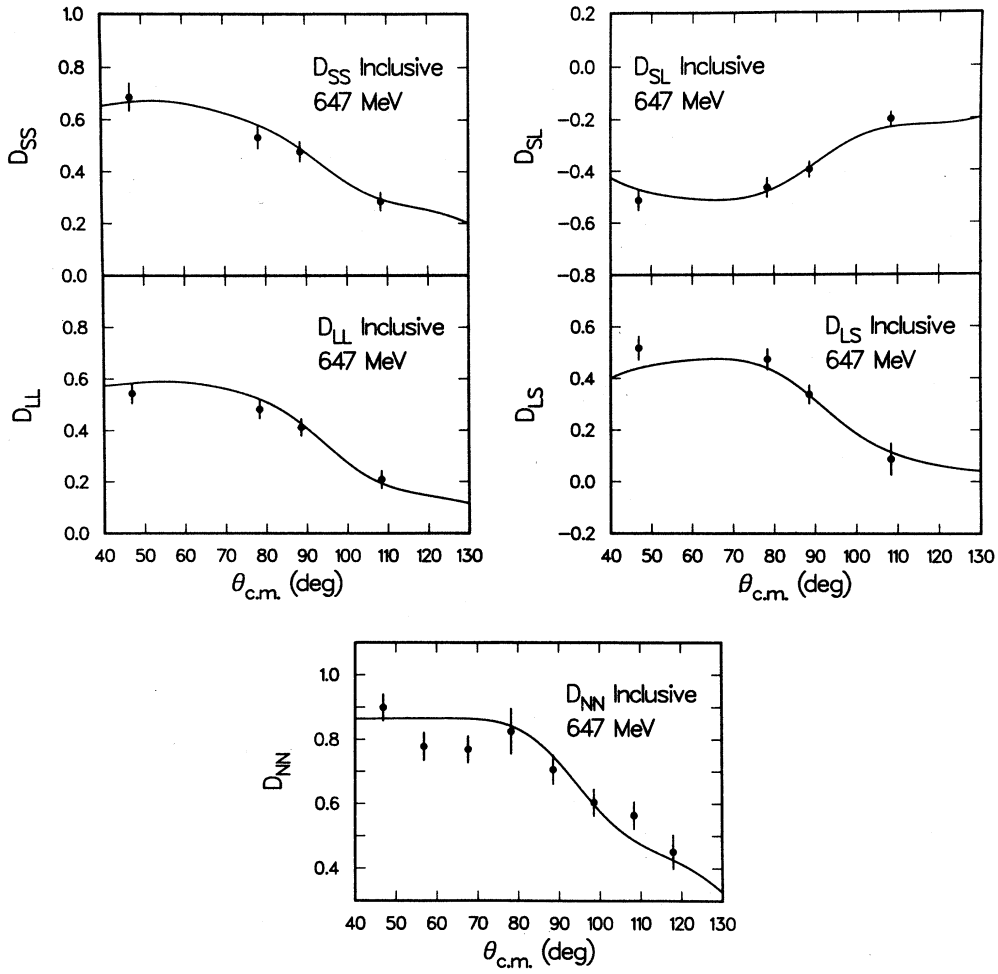

FIG. 3. The spin-rotation depolarization parameters, D_{ij}, for inclusive quasielastic $\vec{p}+{}^2H$ scattering at 647 MeV. The solid curves indicate predictions of the isospin weighting model. The c.m. angles refer to *NN* kinematics as discussed in the text.

III. DATA ANALYSIS AND RESULTS

A. Inclusive quasielastic $\vec{p}+^2$H D_{ij} and A_y parameters

In the off-line analysis events were subjected to a particle (proton) identification test and were restricted to have momentum within a cut set at approximately the full width at half maximum of the quasielastic peak, centered about the momentum of the quasielastic peak. Additional tests insured that each event originated in the deuterium target. Other requirements were placed on particle trajectories through the JANUS polarimeter.[12,14] The proton polarization was computed using the inclusive carbon analyzing power as described in Refs. 12 and 14.

For $\hat{\mathbf{n}}$-type outgoing polarization components there is no precession in the SCYLLA magnetic field. Thus D_{NN}

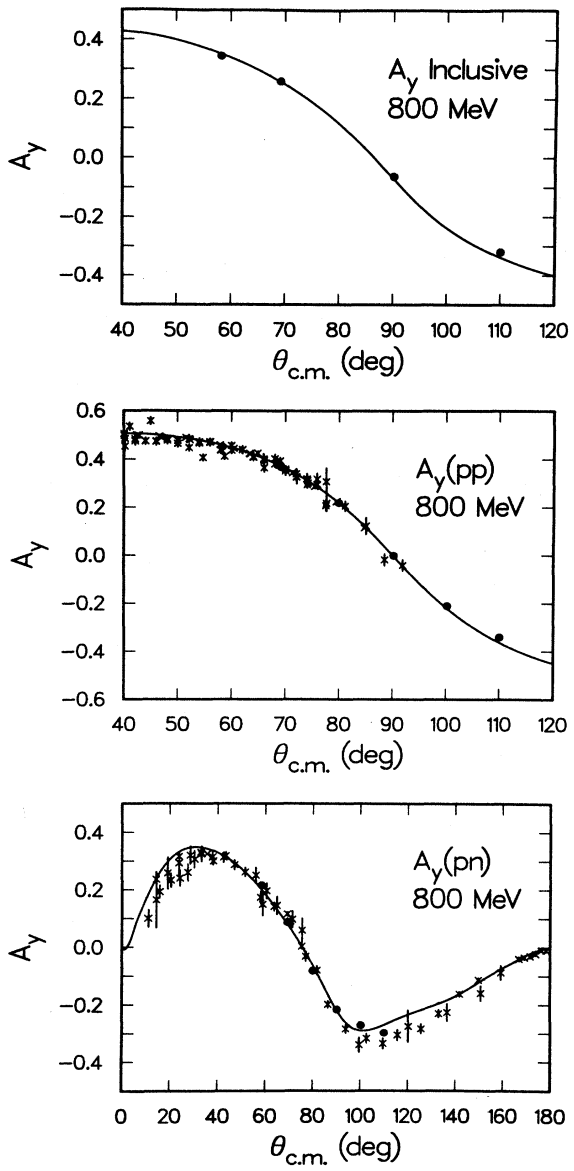

FIG. 4. The 800 MeV inclusive quasielastic $\vec{p}+^2$H and exclusive quasielastic $\vec{p}p$ and $\vec{p}n$ analyzing powers of this experiment (solid dots) are compared with previous data (crosses) from Refs. 10 and 18–26. The analyzing-power data have been renormalized, as discussed in the text. The curves for the *pp* and *pn* analyzing powers are SP87 phase-shift predictions from Ref. 1 while the curve for the inclusive analyzing power is a prediction based on the isospin weighting model and recent phase-shift predictions.

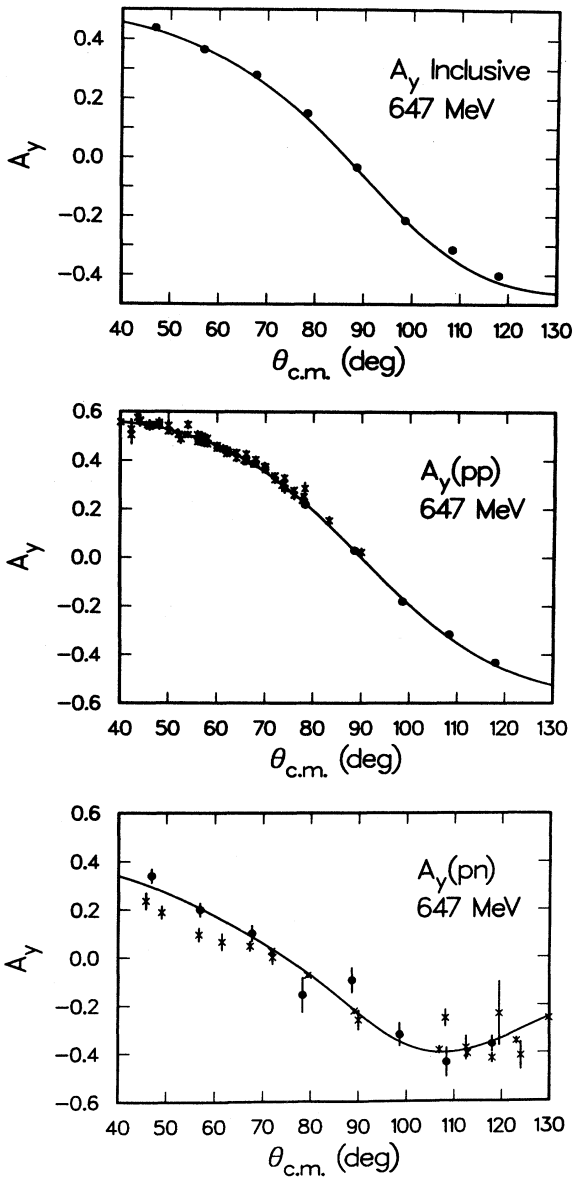

FIG. 5. The 647 MeV inclusive quasielastic $\vec{p}+^2$H and exclusive quasielastic $\vec{p}p$ and $\vec{p}n$ analyzing powers of this experiment (solid dots) are compared with previous data (crosses) from Refs. 1, 18, 19, 25, 27, and 28. The analyzing-power data have been renormalized, as discussed in the text. The curves for the *pp* and *pn* analyzing powers are SP87 phase-shift predictions from Ref. 1 while the curve for the inclusive analyzing power is a prediction based on the isospin weighting model and recent phase-shift predictions.

TABLE III. Exclusive and inclusive quasielastic analyzing powers at 800 MeV. All data have been renormalized by the factor 1.05, as discussed in the text.

Exclusive $\vec{p}p$ and $\vec{p}n$ analyzing powers					
θ_{lab} (deg)	$\theta_{c.m.}$ (deg)	$A_y(\vec{p}p)$	$\Delta A_y(\vec{p}p)$	$A_y(\vec{p}n)$	$\Delta A_y(\vec{p}n)$
25.0	58.3	0.452	±0.010	0.215	±0.010
30.0	69.2	0.368	0.008	0.086	0.010
35.0	79.9	0.219	0.007	−0.083	0.011
40.0	90.2	−0.001	0.007	−0.217	0.012
45.0	100.2	−0.210	0.006	−0.271	0.011
50.0	110.0	−0.340	0.006	−0.298	0.012

Inclusive quasielastic $\vec{p}+^2$H analyzing powers			
θ_{lab} (deg)	$\theta_{c.m.}$ (deg)	A_y	ΔA_y
25.0	58.3	0.345	±0.006
30.0	69.2	0.259	0.006
40.0	90.2	−0.063	0.005
50.0	110.0	−0.320	0.004

is directly related to the $\hat{n}$ polarization component measured with JANUS and is given by the expression

$$D_{NN}=\frac{P^{+}_{\hat{n}'}-P^{-}_{\hat{n}'}}{2P_B(\hat{n})}[1-P_B^2(\hat{n})A_y^2]+A_y^2 ,$$

where $P^{+}_{\hat{n}'}$ ($P^{-}_{\hat{n}'}$) is the measured final-state polarization in the $\hat{n}'$ direction with beam spin normal (reverse), $P_B(\hat{n})$ is the average incident beam polarization in the $\hat{n}$ direction, and A_y is the analyzing power. The above relation is obtained assuming polarization equals analyzing power for quasielastic scattering, $P_B^{+}=-P_B^{-}=P_B$, and no out-of-plane scattering. By computing D_{NN} with the above expression instrumental asymmetries cancel to first order.

Because the horizontal polarization components ($\hat{s}'$ and $\hat{l}'$) precess in SCYLLA, determination of the spin-rotation parameters (D_{SS},D_{SL},D_{LS},D_{LL}) requires measurements at two different precession settings for a given incident-beam spin orientation. In terms of the horizontal spin components determined by JANUS, the spin-rotation parameters may be obtained from the following:

TABLE IV. Exclusive and inclusive quasielastic analyzing powers at 647 MeV. All data have been renormalized by the factor 1.11, as discussed in the text.

Exclusive $\vec{p}p$ and $\vec{p}n$ analyzing powers					
θ_{lab} (deg)	$\theta_{c.m.}$ (deg)	$A_y(\vec{p}p)$	$\Delta A_y(\vec{p}p)$	$A_y(\vec{p}n)$	$\Delta A_y(\vec{p}n)$
20.5	46.9	0.542	±0.011	0.340	±0.031
25.0	56.9	0.474	0.009	0.199	0.030
30.0	67.7	0.388	0.009	0.100	0.035
35.0	78.3	0.220	0.018	−0.157	0.074
40.0	88.6	0.030	0.010	−0.097	0.053
45.0	98.6	−0.180	0.010	−0.323	0.050
50.0	108.4	−0.316	0.011	−0.440	0.062
55.0	118.0	−0.432	0.007	−0.363	0.035

Inclusive quasielastic $\vec{p}+^2$H analyzing powers			
θ_{lab} (deg)	$\theta_{c.m.}$ (deg)	A_y	ΔA_y
20.5	46.9	0.437	±0.007
25.0	56.9	0.365	0.006
30.0	67.7	0.280	0.006
35.0	78.3	0.150	0.013
40.0	88.6	−0.033	0.006
45.0	98.6	−0.214	0.006
50.0	108.4	−0.314	0.007
55.0	118.0	−0.401	0.006

$$D_{XS}=\frac{[(P_\alpha^+-P_\alpha^-)/2P_B^\alpha(\hat{\mathbf{x}})]\overline{\sin\beta}-[(P_\beta^+-P_\beta^-)/2P_B^\beta(\hat{\mathbf{x}})]\overline{\sin\alpha}}{\overline{\cos\alpha}\,\overline{\sin\beta}-\overline{\cos\beta}\,\overline{\sin\alpha}}$$

and

$$D_{XL}=\frac{[(P_\alpha^+-P_\alpha^-)/2P_B^\alpha(\hat{\mathbf{x}})]\overline{\cos\beta}-[(P_\beta^+-P_\beta^-)/2P_B^\beta(\hat{\mathbf{x}})]\overline{\cos\alpha}}{\overline{\sin\alpha}\,\overline{\cos\beta}-\overline{\sin\beta}\,\overline{\cos\alpha}}$$

where $X=S$ or L, $\overline{\sin\alpha}$ and $\overline{\cos\alpha}$ ($\overline{\sin\beta}$ and $\overline{\cos\beta}$) are the event averaged sine and cosine of the precession angle for the first (second) setting, P_α^+ and P_α^- (P_β^+ and P_β^-) are the measured normal and reverse final-state polarizations for the first (second) setting in the horizontal plane, and $P_B^\alpha(\hat{\mathbf{x}})$ [$P_B^\beta(\hat{\mathbf{x}})$] is the average beam polarization in the $\hat{\mathbf{x}}=\hat{\mathbf{s}}$ or $\hat{\mathbf{l}}$ direction for the first (second) setting. In the above equations, it is again assumed that $P_B^+=-P_B^-=P_B$ and the scattering plane is horizontal. The precession angle is computed from trajectory information on an event-by-event basis; the sine and cosine of the precession are then averaged over all events of interest.

The inclusive $\vec{p}+{}^2$H analyzing powers were obtained from the monitor events of the D_{NN} runs since MBD event testing might introduce biases which would alter the relative cross sections. The quasielastic monitor events were required to pass the conjugate trajectory test ("$\phi+\pi$ test" of Refs. 12 and 14) because scattering in the carbon analyzer can produce different effective solid angles for normal and reverse spins if $D_{NN}\neq 0$.

The inclusive quasielastic $\vec{p}+{}^2$H 800 MeV D_{ij} data are shown in Fig. 2 and listed in Table I. The 647 MeV results are given in Fig. 3 and Table II. The 800 and 647 MeV inclusive A_y data are shown in the upper portions of Figs. 4 and 5, respectively, and listed in Tables III and IV, respectively. The 800 and 647 MeV inclusive A_y data were renormalized by the factors 1.05 and 1.11, respec-

TABLE V. Exclusive quasielastic $\vec{p}p$ spin-rotation and -depolarization parameters at 800 MeV.

θ_{lab} (deg)	$\theta_{\text{c.m.}}$ (deg)	D_{NN}	ΔD_{NN}
25.0	58.3	0.865	±0.053
30.0	69.2	0.807	0.053
40.0	90.2	0.679	0.046
45.0	100.2	0.665	0.047
50.0	110.0	0.615	0.043
θ_{lab} (deg)	$\theta_{\text{c.m.}}$ (deg)	D_{SS}	ΔD_{SS}
30.0	69.2	0.539	±0.056
40.0	90.2	0.422	0.070
45.0	100.2	0.486	0.073
50.0	110.0	0.405	0.072
θ_{lab} (deg)	$\theta_{\text{c.m.}}$ (deg)	D_{SL}	ΔD_{SL}
30.0	69.2	−0.325	±0.042
40.0	90.2	−0.392	0.057
45.0	100.2	−0.408	0.058
50.0	110.0	−0.404	0.058
θ_{lab} (deg)	$\theta_{\text{c.m.}}$ (deg)	D_{LL}	ΔD_{LL}
25.0	58.3	0.408	±0.046
30.0	69.2	0.290	0.049
40.0	90.2	0.288	0.040
45.0	100.2	0.204	0.042
50.0	110.0	0.188	0.057
θ_{lab} (deg)	$\theta_{\text{c.m.}}$ (deg)	D_{LS}	ΔD_{LS}
30.0	69.2	0.244	±0.059
40.0	90.2	0.201	0.056
45.0	100.2	0.267	0.061
50.0	110.0	0.247	0.070

TABLE VI. Exclusive quasielastic $\vec{p}p$ spin-rotation and -depolarization parameters at 647 MeV.

θ_{lab} (deg)	$\theta_{\text{c.m.}}$ (deg)	D_{NN}	ΔD_{NN}
20.5	46.9	0.874	±0.058
25.0	56.9	0.722	0.061
30.0	67.7	0.813	0.060
35.0	78.3	0.769	0.103
40.0	88.6	0.702	0.066
45.0	98.6	0.626	0.060
50.0	108.4	0.541	0.063
55.0	118.0	0.542	0.081
θ_{lab} (deg)	$\theta_{\text{c.m.}}$ (deg)	D_{SS}	ΔD_{SS}
20.5	46.9	0.680	±0.084
35.0	78.3	0.505	0.064
40.0	88.6	0.397	0.056
50.0	108.4	0.325	0.056
θ_{lab} (deg)	$\theta_{\text{c.m.}}$ (deg)	D_{SL}	ΔD_{SL}
20.5	46.9	−0.391	±0.059
35.0	78.3	−0.452	0.057
40.0	88.6	−0.304	0.044
50.0	108.4	−0.232	0.043
θ_{lab} (deg)	$\theta_{\text{c.m.}}$ (deg)	D_{LL}	ΔD_{LL}
20.5	46.9	0.533	±0.058
35.0	78.3	0.357	0.050
40.0	88.6	0.273	0.048
50.0	108.4	0.078	0.052
θ_{lab} (deg)	$\theta_{\text{c.m.}}$ (deg)	D_{LS}	ΔD_{LS}
20.5	46.9	0.392	±0.068
35.0	78.3	0.399	0.061
40.0	88.6	0.271	0.053
50.0	108.4	−0.018	0.100

tively, as discussed in the next subsection. The data were averaged over the full laboratory acceptance of the apparatus ($\sim\pm 2°$). The center-of-momentum angle for each data point was computed for the central angle of the apparatus using elastic NN kinematics, but accounting for the 2.2 MeV binding energy of the deuteron.

B. Exclusive quasielastic D_{ij} and A_y parameters

Exclusive quasielastic $\vec{p}p$ D_{ij} data were obtained simultaneously with the inclusive data, using information from the recoil-particle detection system. Exclusive scattering events were required to pass the same cuts and restrictions as the inclusive data with the additional requirement that only JANUS events which had a recoil proton associated with them were accepted. Recoil protons were identified as events that registered in both a charged-particle detector and a detector of the recoil array[8] and that were correlated in time with respect to the JANUS event. Spin observables were computed as described previously.

The 800 MeV quasielastic $\vec{p}p$ D_{ij} data are listed in Table V and are shown in Fig. 6 where they are compared with previously measured elastic[12,15,16] and quasielastic[8] $\vec{p}p$ results and recent phase-shift predictions.[1] The 647 MeV quasielastic $\vec{p}p$ D_{ij} data are given in Table VI and shown in Fig. 7, along with previous elastic $\vec{p}p$ results[1,15,17] and SP87 phase-shift predictions.[1] Agreement among the previous $\vec{p}p$ data and the quasielastic results of this experiment is generally good and indicates that exclusive quasielastic spin measurements at these energies and momentum transfers provide accurate representations of elastic NN spin observables.

For the exclusive quasielastic $\vec{p}p$ and $\vec{p}n$ analyzing-power measurements a recoil proton or neutron[8] was required to be in coincidence with the forward-scattered proton. For the 800 MeV exclusive A_y measurements data were also obtained with the carbon analyzer of the JANUS polarimeter removed and without MBD testing. Exclusive quasielastic $\vec{p}p$ analyzing-power data from the D_{NN} runs using monitor events and those from runs without the carbon analyzer agreed to within the statistical uncertainties of the measurements ($\pm 0.01-0.02$). An insufficient event rate and running time prevented ex-

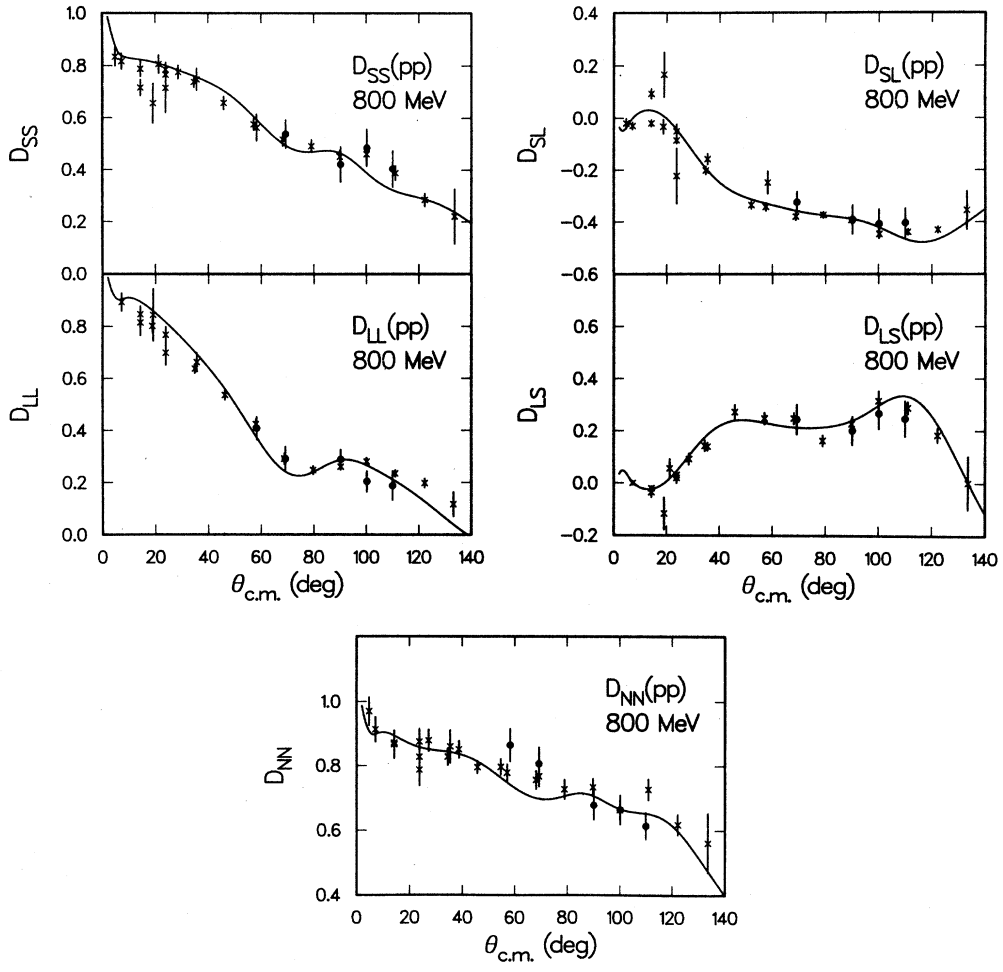

FIG. 6. The 800 MeV exclusive quasielastic $\vec{p}p$ D_{ij} results of this experiment (solid dots) are compared with previous data (crosses) from Refs. 8, 12, 15, and 16 and with the SP87 phase-shift predictions (solid curves) of Ref. 1.

clusive quasielastic $\vec{p}n$ D_{ij} data from being obtained in this experiment.

The exclusive A_y data are listed in Tables III and IV and shown in Figs. 4 and 5 in comparison with recent phase-shift predictions[1] and with existing data from Refs. 10 and 18–26 for 800 MeV and Refs. 1, 18,19, 25, 27, and 28 for 647 MeV. At both 800 and 647 MeV, the exclusive $\vec{p}p$ analyzing powers were found to be systematically smaller than either the existing data or the phase-shift predictions. Renormalization factors of 1.05 and 1.11 provided the best agreement with previous pp data and phase-shift predictions at 800 and 647 MeV, respectively. These renormalizations were applied to all 800 and 647 MeV analyzing-power data presented here and are included in both the tabulated data and the figures.

The cause of the normalization discrepancy is not understood, but possibly originates from uncertainties in the normalizations of the relative spin-up and spin-down cross sections. This could be due to miscalculation of detector efficiencies and/or system dead times for the two incident spin directions. An uncertainty of this type is supported by the larger normalization factor required at 647 MeV, where the LAMPF accelerator duty factor is 3 times less than at 800 MeV. Additionally, the good agreement seen between the quasielastic $\vec{p}p$ D_{ij} measurements of this experiment and previous elastic $\vec{p}p$ measurements supports the conclusion that the systematic discrepancies in the analyzing-power measurements are *not* due to incident-beam polarization uncertainties or misidentification of recoil particles.

The 800 MeV quasielastic $\vec{p}p$ analyzing powers (with renormalization factor) are in good agreement with the existing data and the SP87 phase-shift prediction. The 800 MeV quasielastic $\vec{p}n$ analyzing powers are also well described by the phase-shift prediction and follow the trends of the existing data sets, although there appears to be a slight difference between the data sets near the minimum in the analyzing power at 100° c.m. Similarly the 647 MeV exclusive analyzing-power data of this experiment are adequately described by recent phase-shift predictions (with data renormalization factor) and are consistent with previous data as shown in Fig. 5.

C. Isospin weighting model

The inclusive $\vec{p}+{}^2$H spin observables were compared with predictions of a simple isospin weighting model.

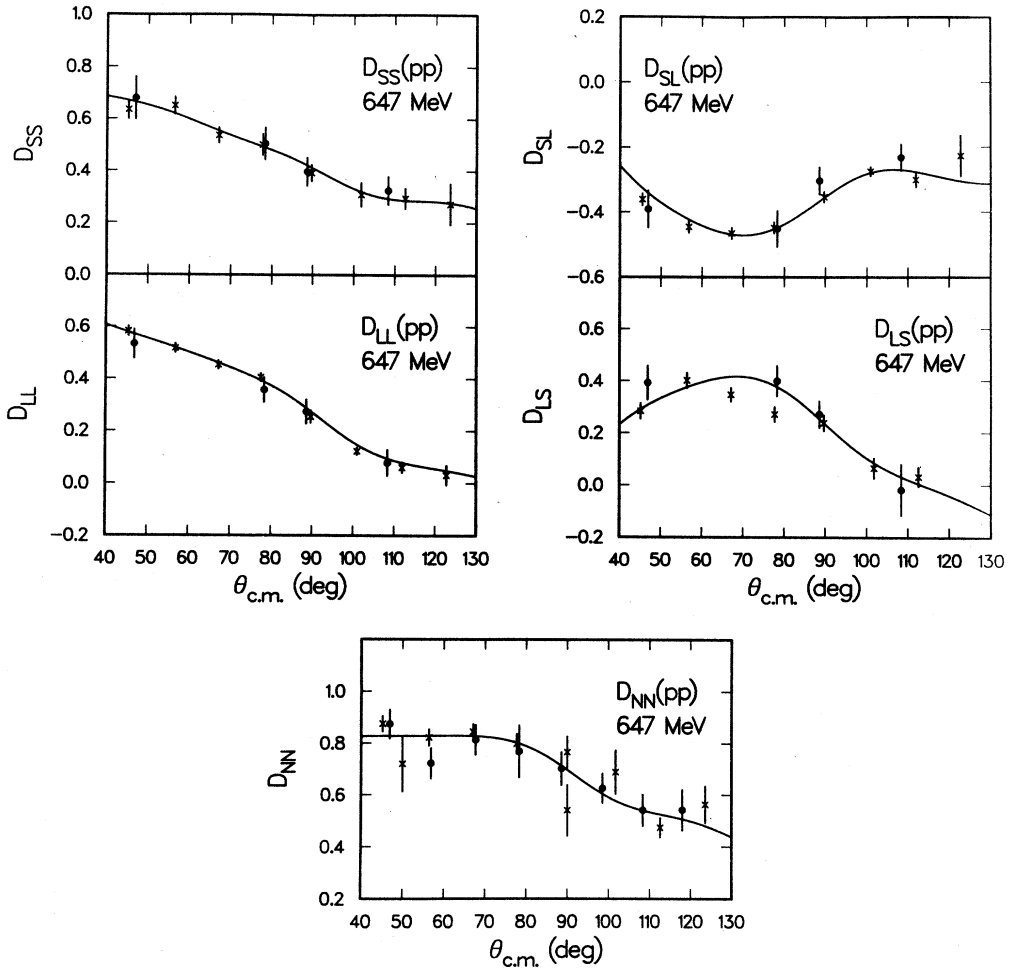

FIG. 7. The 647 MeV exclusive quasielastic $\vec{p}p$ D_{ij} results of this experiment (solid dots) are compared with previous data (crosses) from Refs. 1, 15, and 17 and with the SP87 phase-shift predictions (solid curves) of Ref. 1.

Based on the success of this model estimates for the quasielastic $\vec{p}n$ D_{ij} observables were deduced from the inclusive data.

The model assumes that the inclusive quasielastic spin-dependent differential cross sections are proportional to the sum of the exclusive *pp* and *pn* quasielastic spin-dependent differential cross sections. From this it follows that the inclusive quasielastic spin observable X_I can be expressed as

$$X_I = \frac{\sigma_{pp}^{\mathrm{ex}}}{\sigma_{pp}^{\mathrm{ex}}+\sigma_{pn}^{\mathrm{ex}}} X_{pp}^{\mathrm{ex}} + \frac{\sigma_{pn}^{\mathrm{ex}}}{\sigma_{pp}^{\mathrm{ex}}+\sigma_{pn}^{\mathrm{ex}}} X_{pn}^{\mathrm{ex}} ,$$

where $\sigma_{pp}^{\mathrm{ex}}$ ($\sigma_{pn}^{\mathrm{ex}}$) is the exclusive *pp* (*pn*) differential cross section at the appropriate angle and X_{pp}^{ex} (X_{pn}^{ex}) is the exclusive quasielastic *pp* (*pn*) spin observable corresponding to X_I. One can see that if X_I, X_{pp}^{ex}, and $\sigma_{pp}^{\mathrm{ex}}/\sigma_{pn}^{\mathrm{ex}}$ are known, then X_{pn}^{ex} may be calculated. Since the experiment determined X_I and X_{pp}^{ex}, only the relative cross section ratio, $\sigma_{pp}^{\mathrm{ex}}/\sigma_{pn}^{\mathrm{ex}}$, must be determined in order to deduce X_{pn}^{ex}. In addition, the results in Refs. 8 and 9 and Figs. 4–7 indicate that X_{pp}^{ex} and X_{pn}^{ex} are very close to the free *NN* values.

Model predictions using the SP87 free *NN* observables of Arndt[1] are compared with the inclusive D_{ij} and A_y data in Figs. 2–5. The good agreement between the predictions (solid curves) and data supports the general assumptions of the isospin weighting model, indicates that ($\sigma_{pp}^{\mathrm{ex}}/\sigma_{pn}^{\mathrm{ex}}$) is well represented by the ratio of the SP87 free *NN* cross sections, and suggests that the $\vec{p}n$ D_{ij} observables are reasonably described by the SP87 phase-shift predictions. The model reproduces the inclusive A_y data especially well where it is significant to note that the *NN* phase-shift predictions used as input provide very good descriptions of the $\vec{p}p$ and $\vec{p}n$ analyzing powers (see Figs. 4 and 5).

The model was next used to deduce exclusive quasielastic $\vec{p}n$ D_{ij} observables from the inclusive data. The ratio of the exclusive *pp* and *pn* cross sections was obtained from the model at each angle using the inclusive and exclusive analyzing-power data from this experiment (except at $\theta_{\mathrm{lab}}=45°$ at 800 MeV, where the inclusive analyz-

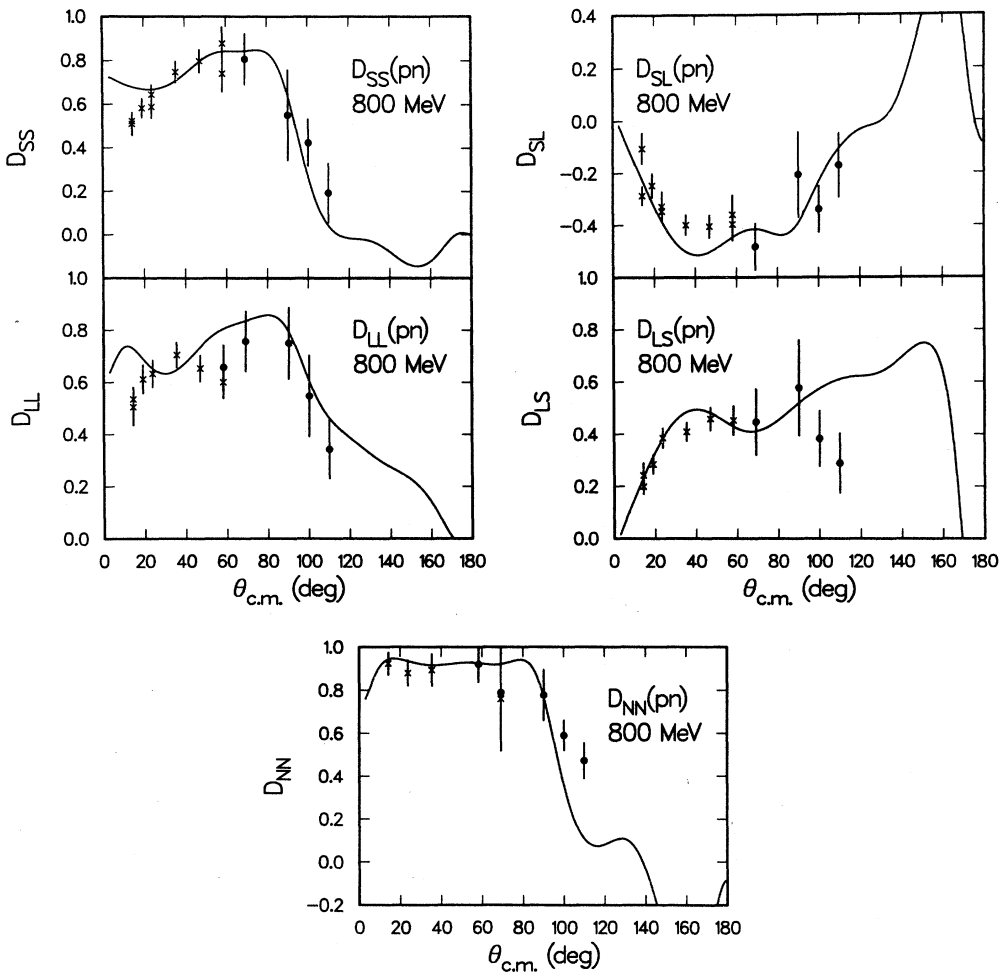

FIG. 8. The 800 MeV *pn* D_{ij}'s (solid dots) deduced using the isospin weighting model and data from this experiment are compared with previous data (crosses) from Ref. 8 and SP87 phase-shift predictions of Ref. 1.

ing power was calculated with the model using SP87 phase-shift predictions[1] as input and at $\theta_{lab}=50°$ at 647 MeV, where the phase shift cross section ratio was used).

The deduced 800 MeV *pn* D_{ij} values are shown in Fig. 8, along with existing exclusive quasielastic *pn* data[8] and the SP87 phase-shift predictions.[1] The values are listed in Table VII. The deduced *pn* spin parameters are in good agreement with the previous data in the region of overlap but differ quantitatively from the phase-shift predictions, particularly for the parameters D_{NN} and D_{LS} at the largest angles. This is in contrast to the exclusive *pp* measurements for these spin observables, where at large angles the data are in good agreement with both the existing data and phase-shift predictions.

The 647 MeV deduced *pn* D_{ij}'s are given in Table VIII and shown in Fig. 9 in comparison with SP87 phase-shift predictions. The phase-shift analysis reproduces the overall magnitudes of the deduced observables but quantitative comparisons are not possible given the large statistical uncertainty in the deduced quantities.

Additional spin-dependent *pn* measurements are necessary before definitive statements can be made concerning the accuracy of the $I=0$ components of the *NN* amplitudes at and above 650 MeV. The quantitative disagreement shown in Fig. 8 lends support to the belief that there is need for improvement in the empirical $I=0$ phases above 500 MeV.[29]

IV. EXPERIMENTAL UNCERTAINTIES

The errors quoted for the inclusive quasielastic $\vec{p}+{}^2$H and exclusive quasielastic $\vec{p}p$ D_{ij} data (Tables I, II, V, and VI) include both the statistical uncertainty associated with the determination of the final-state polarization and the statistical uncertainty of the measured incident-beam polarization. In addition, a principal source of systematic error in these measurements is that associated with the parametrized inclusive $\vec{p}+{}^{12}$C analyzing power used in calculating the final-state polarization.[11] This error, $<\pm 2\%$, has been included in the quoted uncertainty as a

TABLE VII. Deduced quasielastic *pn* spin-rotation and -depolarization parameters at 800 MeV.

θ_{lab} (deg)	$\theta_{c.m.}$ (deg)	D_{NN}	ΔD_{NN}
25.0	58.3	0.920	±0.085
30.0	69.2	0.789	0.100
40.0	90.2	0.777	0.120
45.0	100.2	0.590[a]	0.072[a]
50.0	110.0	0.472	0.085
θ_{lab} (deg)	$\theta_{c.m.}$ (deg)	D_{SS}	ΔD_{SS}
30.0	69.2	0.808	±0.118
40.0	90.2	0.551	0.210
45.0	100.2	0.425[a]	0.110[a]
50.0	110.0	0.193	0.139
θ_{lab} (deg)	$\theta_{c.m.}$ (deg)	D_{SL}	ΔD_{SL}
30.0	69.2	−0.483	±0.091
40.0	90.2	−0.207	0.165
45.0	100.2	−0.339[a]	0.091[a]
50.0	110.0	−0.171	0.125
θ_{lab} (deg)	$\theta_{c.m.}$ (deg)	D_{LL}	ΔD_{LL}
25.0	58.3	0.658	±0.087
30.0	69.2	0.758	0.118
40.0	90.2	0.751	0.139
45.0	100.2	0.548[a]	0.158[a]
50.0	110.0	0.343	0.114
θ_{lab} (deg)	$\theta_{c.m.}$ (deg)	D_{LS}	ΔD_{LS}
30.0	69.2	0.446	±0.129
40.0	90.2	0.577	0.185
45.0	100.2	0.383[a]	0.108[a]
50.0	110.0	0.289	0.116

[a]Calculated using the inclusive analyzing power from the isospin weighting model with SP87 *NN* phase-shift (Ref. 1) input as discussed in the text.

TABLE VIII. Deduced quasielastic *pn* spin-rotation and -depolarization parameters at 647 MeV.

θ_{lab} (deg)	$\theta_{c.m.}$ (deg)	D_{NN}	ΔD_{NN}
20.5	46.9	0.922	±0.062
25.0	56.9	0.863	0.104
30.0	67.7	0.696	0.106
35.0	78.3	1.071	0.501
40.0	88.6	0.710	0.084
45.0	98.6	0.534	0.206
50.0	108.4	0.646[a]	0.237[a]
55.0	118.0	0.339	0.174
θ_{lab} (deg)	$\theta_{c.m.}$ (deg)	D_{SS}	ΔD_{SS}
20.5	46.9	0.694	±0.102
35.0	78.3	0.650	0.300
40.0	88.6	0.560	0.105
50.0	108.4	0.142[a]	0.226[a]
θ_{lab} (deg)	$\theta_{c.m.}$ (deg)	D_{SL}	ΔD_{SL}
20.5	46.9	−0.626	±0.085
35.0	78.3	−0.522	0.266
40.0	88.6	−0.488	0.101
50.0	108.4	−0.095[a]	0.175[a]
θ_{lab} (deg)	$\theta_{c.m.}$ (deg)	D_{LL}	ΔD_{LL}
20.5	46.9	0.552	±0.071
35.0	78.3	1.030	0.331
40.0	88.6	0.553	0.141
50.0	108.4	0.678[a]	0.231[a]
θ_{lab} (deg)	$\theta_{c.m.}$ (deg)	D_{LS}	ΔD_{LS}
20.5	46.9	0.632	±0.100
35.0	78.3	0.798	0.323
40.0	88.6	0.404	0.097
50.0	108.4	0.463[a]	0.454[a]

[a]Calculated using *pp*/*pn* cross section ratio from phase-shift solution SP87 (Ref. 1) as discussed in the text.

point-to-point normalization error. For the deduced *pn* spin-rotation depolarization data (Tables VII and VIII), the errors include contributions associated with uncertainties in the inclusive $\vec{p}+{}^2\mathrm{H}$ and exclusive $\vec{p}\vec{p}$ measurements as well as the deduced *pp*/*pn* cross section ratios. The errors for the analyzing powers (Tables III and IV) include statistical contributions from both the measured asymmetries and the determination of the incident-beam polarization.

Other experimental errors have been evaluated but have not been included in the tabulated errors. These include the uncertainty in the absolute beam polarization ($\pm 1\%$) (Ref. 18) common to all polarized-beam experiments at LAMPF, target flask and vacuum window contributions to the measured observables (estimated at $<\pm 2\%$), and other sources of error which are believed to be negligible for this experiment.[30] The good agreement between the exclusive quasielastic $\vec{p}\vec{p}$ D_{ij} data of this experiment and previous elastic *pp* measurements implies that these additional sources of error are insignificant. Thus the total experimental uncertainty not included in the quoted errors is believed to be $<\pm 0.03$ and represents the absolute normalization uncertainty of the data sets from this experiment.

V. SUMMARY AND CONCLUSIONS

We have presented new 647 and 800 MeV inclusive quasielastic $\vec{p}+{}^2\mathrm{H}$ analyzing-power and spin-rotation depolarization data spanning the center-of-momentum angular ranges 46.9°–118.0° and 58.3°–110.0°, respectively. We have also presented 647 and 800 MeV exclusive quasielastic $\vec{p}\vec{p}$ and $\vec{p}\vec{n}$ analyzing-power data and exclusive $\vec{p}\vec{p}$ spin-rotation depolarization data which were obtained in conjunction with the inclusive measurements. The *pp* analyzing-power data, after renormalization, were found to be in good agreement with previous measurements; the *pn* analyzing powers are in general agreement with recent phase-shift predictions, but the 800 MeV data disagree with existing data near the minimum in the analyzing power. The exclusive quasielastic $\vec{p}\vec{p}$ D_{ij} data are in good agreement with previous elastic *pp* measurements indicating that the quasielastic data provide

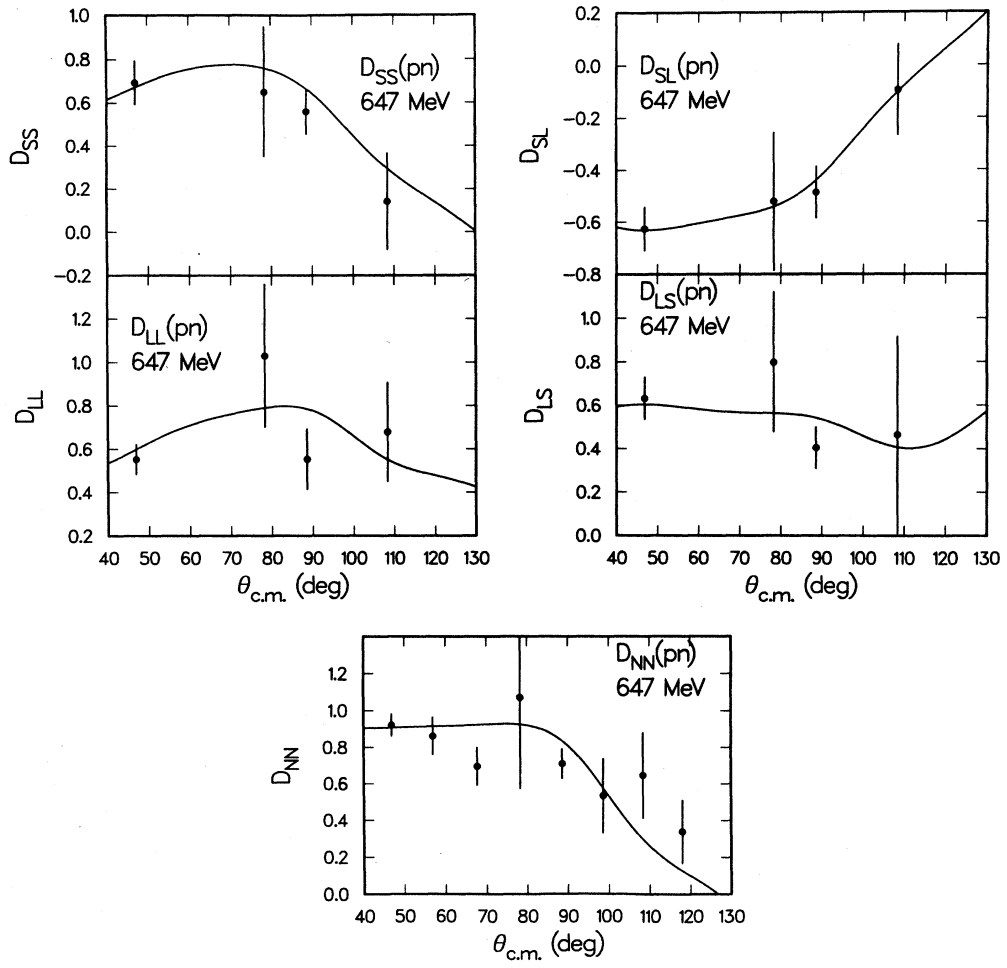

FIG. 9. The 647 MeV *pn* D_{ij}'s (solid dots) deduced using the isospin weighting model and data from this experiment are compared with the SP87 phase-shift predictions of Ref. 1.

reasonable representations of the free *NN* values.

A simple isospin weighting model was presented which relates the exclusive and inclusive quasielastic spin observables. Good descriptions of the inclusive D_{ij} and A_y data were obtained with it. The model was then used to deduce *pn* spin-rotation depolarization observables. The 800 MeV deduced *pn* observables agreed with previous data in the region of overlap. Both the 800 and 647 MeV deduced results compare favorably with recent phase-shift predictions, but quantitative differences between some of the deduced observables and the phase-shift predictions suggest that there is room for improvement in our knowledge of the $I=0$ *NN* amplitudes at higher energies.

The isospin weighting model was shown to provide an expedient means for studying *pn* elastic scattering in that one only needs to obtain the relatively simple, one-arm inclusive quasielastic $\vec{p}+{}^2$H spin data (given accurate *pp* data). Such information can help fill the present void in the *pn* data base above 500 MeV until an adequate amount of free *pn* spin-observable data can be measured.

This work was supported in part by the U.S. Department of Energy and The Robert A. Welch Foundation.

---

*Present address: Department of Physics, University of Udine, Italy.

†Present address: Lockheed Missiles and Space Corp., Sunnyvale, CA 94088.

‡Present address: Argonne National Laboratory, Argonne, Illinois 60439.

[1]R. A. Arndt, J. S. Hyslop III, and L. D. Roper, Phys. Rev. D **35**, 128 (1987); Scattering Analysis Interactive Dialin (SAID), R. A. Arndt and D. Roper, Virginia Polytechnic Institute and State University, and references contained in SAID database.

[2]G. R. Burleson *et al.*, Phys. Rev. Lett. **59**, 1645 (1987).

[3]S. Nath *et al.*, Phys. Rev. D **39**, 3520 (1989).

[4]A. K. Kerman, H. McManus, and R. M. Thaler, Ann. Phys. (N.Y.) **8**, 551 (1959).

[5]L. Ray, Phys. Rev. C **19**, 1855 (1979).

[6]J. A. McNeil, J. Shepard, and S. J. Wallace, Phys. Rev. Lett. **50**, 1439 (1983); **50**, 1443 (1983).

[7]B. C. Clark, S. Hama, R. L. Mercer, L. Ray, and B. D. Serot, Phys. Rev. Lett. **50**, 1644 (1983).

[8]M. L. Barlett *et al.*, Phys. Rev. C **32**, 239 (1985).

[9]J. A. Marshall, M. L. Barlett, R. W. Fergerson, G. W. Hoffmann, E. C. Milner, L. Ray, J. F. Amann, B. E. Bonner, and J. B. McClelland, Phys. Rev. C **34**, 1433 (1986).

[10]M. W. McNaughton, P. R. Bevington, H. B. Willard, E. Winkelmann, E. P. Chamberlin, F. H. Cverna, N. S. P. King, and H. Willmes, Phys. Rev. C **23**, 1128 (1981).

[11]R. D. Ransome *et al.*, Nucl. Instrum. Methods **201**, 315 (1982); D. J. Cremins, M.S. thesis, The University of Texas at Austin, 1983.

[12]M. W. McNaughton, B. E. Bonner, W. D. Cornelius, E. W. Hoffman, O. B. van Dyck, R. L. York, R. D. Ransome, C. L. Hollas, P. J. Riley, and K. Toshioka, Phys. Rev. C **25**, 1967 (1982).

[13]D. Besset, B. Favier, L. G. Greeniaus, R. Hess, C. Lechanoine, D. Rapin, and D. W. Werren, Nucl. Instrum. Methods **166**, 515 (1979).

[14]R. D. Ransome, S. J. Greene, C. L. Hollas, B. E. Bonner, M. W. McNaughton, C. L. Morris, and H. A. Thiessen, Nucl. Instrum. Methods **201**, 309 (1982).

[15]C. L. Hollas *et al.*, Phys. Rev. C **30**, 1251 (1984).

[16]M. L. Barlett, G. W. Hoffmann, J. A. McGill, R. W. Fergerson, E. C. Milner, J. A. Marshall, J. F. Amann, B. E. Bonner, and J. B. McClelland, Phys. Rev. C **30**, 279 (1984).

[17]M. W. McNaughton *et al.*, Phys. Rev. C **26**, 249 (1982).

[18]M. W. McNaughton and E. P. Chamberlin, Phys. Rev. C **24**, 1778 (1981).

[19]J. Bystricky *et al.*, Nucl. Phys. **B262**, 727 (1985).

[20]M. L. Barlett *et al.*, Phys. Rev. C **27**, 682 (1983).

[21]P. R. Bevington *et al.*, Phys. Rev. Lett. **41**, 384 (1978).

[22]D. A. Bell *et al.*, Phys. Lett. **94B**, 310 (1980).

[23]J. Bystricky *et al.*, Nucl. Phys. **A444**, 597 (1985).

[24]R. D. Ransome *et al.*, Phys. Rev. Lett. **48**, 781 (1982).

[25]G. A. Korolev, A. V. Khanzadeev, G. E. Petrov, E. M. Spiridenkov, A. A. Vorobyov, Y. Terrien, J. C. Lugol, J. Saudinos, B. H. Silverman, and F. Wellers, Phys. Lett. **165B**, 262 (1985).

[26]C. Newsom, Ph.D. thesis, The University of Texas at Austin, 1980; C. R. Newsom *et al.*, Phys. Rev. C **39**, 965 (1989).

[27]M. W. McNaughton, E. P. Chamberlin, J. J. Jarmer, N. S. P. King, H. B. Willard, and E. Winkelman, Phys. Rev. C **25**, 2107 (1982).

[28]R. Zulkarneev, Kh. Murtazaev, and V. Khachaturov, Phys. Lett. **61B**, 164 (1976).

[29]R. A. Arndt, Phys. Rev. D **37**, 2665 (1988).

[30]These additional sources of error are due to uncertainties in the precession angle for the spin-rotation measurements, out-of-plane (nonhorizontal) scattering effects, corrections for small components of other beam spin orientations in the measurements, false or instrumental asymmetries, and recoil-particle misidentification in the exclusive measurements.